

Efficiency Calculation and Configuration Design of a PEM Electrolyzer System for Hydrogen Production

Houcheng Zhang, Shanhe Su, Guoxing Lin^{*}, Jincan Chen^{**}

Department of Physics, Xiamen University, Xiamen 361005, People's Republic of China

^{*}E-mail: gxlin@xmu.edu.cn

^{**}E-mail: jcchen@xmu.edu.cn

Received: 23 March 2012 / *Accepted:* 14 April 2012 / *Published:* 1 May 2012

A PEM electrolyzer system for hydrogen production is established and the corresponding efficiency is derived. Based on semi-empirical equations, thermodynamic-electrochemical modeling of water splitting reaction is systematically carried out. It is confirmed that the Joule heat resulting from the irreversibilities inside the PEM electrolyzer is larger than that needed in the water splitting process in the whole region of the electric current density. Some alternative configurations are designed to improve the overall performance of the system and the corresponding expressions of the efficiency are also derived. The curves of the efficiency varying with the electric current density are presented and the efficiencies of the different configurations are compared. The optimally operating region of the electric current density is determined. The effects of some of the important parameters on the performance of the PEM electrolyzer system are analyzed in detail. Some significant results for the optimum design strategies of a practical PEM electrolyzer system for hydrogen production are obtained.

Keywords: PEM electrolyzer system; hydrogen production; efficiency calculation; configuration design; performance analysis.

1. INTRODUCTION

Hydrogen has been considered as an ideal energy carrier to support sustainable energy development, which can be effectively produced based on fossil-fuel-based processes, e.g. ethanol, methane and natural gas reforming [1-5]. However, the development of renewable hydrogen production technologies to replace fossil fuel-based hydrogen production methods is an important step towards a sustainable hydrogen economy [6-9].

Water electrolysis integrated with clean energy sources such as nuclear power stations, photovoltaics or wind turbines is a more practical technology for large-scale renewable hydrogen

production. Up until now, most of the research and development on water electrolysis related to renewable hydrogen production projects have focused on alkaline electrolysis systems and PEM electrolyzers. Compared with traditional alkaline electrolysis systems, PEM electrolyzers are more advantageous due to their ecological cleanness, easy maintenance, compactness, etc.[10, 11] Recently, most studies on PEM electrolysis emphasize on the development of new catalysts [12-15], cell and stack assembly for high efficiencies [16-19]. Comparatively, the detailed heat recovery strategies on systematical efficiency and performance analysis are rarely investigated, which is worthwhile to be further studied.

In the present paper, a PEM electrolyzer system is established and the efficiencies of the system are presented for differently operating conditions. Based on semi-empirical equations, thermodynamic-electrochemical modeling of the electrolysis process is systematically carried out, where multi-irreversibilities inside the system are taken into account. In order to improve the performance of the system, some alternative configurations for utilizing the redundant heat produced in the PEM electrolyzer are put forward. The efficiencies of these configurations are derived and the lower boundary of the operating current density is determined. The effects of some of the important parameters such as the operating temperature, electrolyte membrane thickness, effectiveness of heat exchangers, and inlet flow rate of H₂O on the performance of the PEM electrolyzer system are analyzed in detail.

2. THE EFFICIENCIES OF A PEM ELECTROLYZER SYSTEM

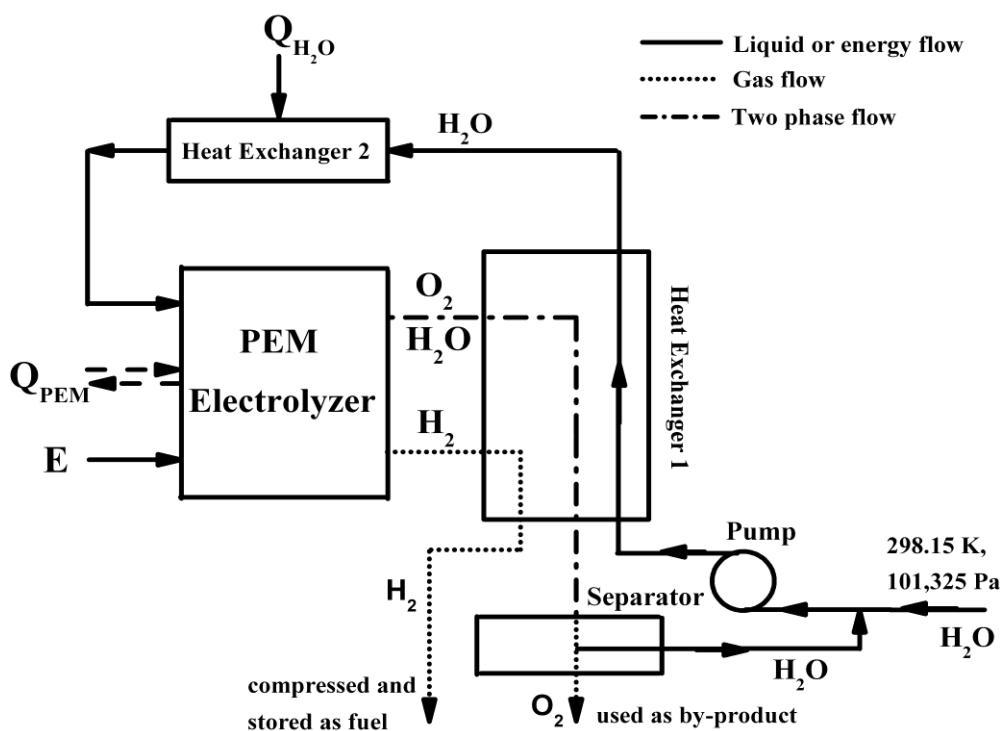


Figure 1. The schematic diagram of a PEM electrolyzer system for hydrogen production.

Figure 1 shows the schematic diagram of a PEM electrolyzer system for hydrogen production. The system is mainly composed of a PEM electrolyzer, a separator, a pump and two heat exchangers. In order to drive the water splitting reactions, water, electricity and heat, if necessary, are provided to the PEM electrolyzer. The generated H₂ flows out at the cathode and the generated O₂ and residual H₂O flow out at the anode. The waste heat remained in the products at the outlet can be utilized through the use of heat exchanger 1. After leaving heat exchanger 1, H₂ is cooled down to reference condition (298.15 K and 101,325 Pa), compressed and stored as fuel. The O₂/H₂O mixture flows into the separator, O₂ is cooled down and can be used as by-product; and the hot H₂O is circulated in the H₂O supply stream at reference condition and pumped into heat exchanger 1 for the next H₂ production cycle. Due to the different thermodynamic parameters of reactants/products and the inefficiency of heat exchanger 1, the feeding water should be further heated through heat exchanger 2 before reaching the temperature of the PEM electrolyzer. Such a model is more general and reasonable than the conventional ones [20] as it includes main energy consumption processes of hydrogen production and the waste heat produced in the electrolyzer can be efficiently utilized.

According to Fig. 1, the efficiency of the PEM electrolyzer system for hydrogen production can be expressed as

$$\eta_T = \frac{N_{H_2,out} LHV \eta_{H_2}}{E + Q_{PEM} (1 - \frac{T_0}{T_x}) + Q_{H_2O} (1 - \frac{T_0}{T_s})}, \tag{1a}$$

where $N_{H_2,out}$ is the outlet flow rate of H₂; LHV is the lower heating value of H₂; E is the electric energy input; Q_{PEM} is the thermal energy provided to the PEM electrolyzer or released to the environment, Q_{H_2O} is the thermal energy input to the second heat exchanger for further heating up H₂O, T_0 and T_s are, respectively, the temperatures of the environment and external heat source supplying heat for heating up H₂O, T_x is the temperature of the external heat source, the PEM electrolyzer, or the environment and depends on the sign of Q_{PEM} , $\eta_{H_2} = 1 - T_0/T_H$, and T_H is the combustion temperature of H₂ at reference condition. Because T_H is independent of the parameters of the PEM electrolyzer system, one can simply give another definition of the efficiency as

$$\eta = \eta_T / \eta_{H_2} = \frac{N_{H_2,out} LHV}{E + Q_{PEM} (1 - \frac{T_0}{T_x}) + Q_{H_2O} (1 - \frac{T_0}{T_s})}. \tag{1b}$$

Equation (1a) or (1b) may be used to calculate the efficiency of a PEM electrolyzer system for hydrogen production. The results obtained only have a constant difference which is independent of the parameters of the system. Below, we directly use Eq. (1b) to calculate the efficiency of the system for simplicity.

When $Q_{PEM} \geq 0$, $T_x = T_s$ and Eq. (1b) can be directly written as

$$\eta = \frac{N_{H_2,out} LHV}{E + Q_{PEM} \left(1 - \frac{T_0}{T_s}\right) + Q_{H_2O} \left(1 - \frac{T_0}{T_s}\right)} \quad (2)$$

When $Q_{PEM} < 0$ and the redundant heat $|Q_{PEM}|$ resulting from the PEM electrolyzer is directly released to environment, $T_x = T_0$ and Eq. (1b) can be simplified as

$$\eta = \frac{N_{H_2,out} LHV}{E + Q_{H_2O} \left(1 - \frac{T_0}{T_s}\right)} \quad (3)$$

It is worthwhile to note that if the redundant heat $|Q_{PEM}|$ resulting from the PEM electrolyzer is utilized, one can improve the performance of the PEM electrolyzer system. We will specially discuss this problem in the next few sections.

It should be pointed out that for a practical electrolyzer system for hydrogen production; the hydrogen storage and the operation of some auxiliaries usually consume some additional energy. For the sake of calculative convenience, the additional energy is not considered in Eqs. (1)-(3) because it is small compared with the input electric energy of the electrolyzer.

3. THE ALTERNATIVE CONFIGURATIONS OF A PEM ELECTROLYZER SYSTEM AND THEIR EFFICIENCIES

Many researchers have elaborately demonstrated the operating mechanism of a PEM electrolyzer system for hydrogen production [11, 21-23]. Here, we only give a simple description. As shown in Fig. 1, the overall water splitting reaction is that H_2O plus electricity and heat turns to H_2 and O_2 , i.e., $H_2O + \text{heat} + \text{electricity} \rightarrow H_2 + 0.5O_2$. The total energy required for electrolytic hydrogen production $\Delta H(T)$ is given by

$$\Delta H(T) = Q(T) + \Delta G(T), \quad (4)$$

where $\Delta G(T)$ is the electrical energy demand, i.e., the change in the Gibbs free energy, $Q(T) = T\Delta S(T)$ is the thermal energy demand, $\Delta S(T)$ is the entropy change in the water splitting reaction process, and T is the operating temperature of the PEM electrolyzer.

According to Refs. [24-27], the reversible voltage of a PEM water electrolysis process can be determined by Nernst equation, i.e.,

$$V_0 = 1.229 - 8.5 \times 10^{-4} (T - T_0) + 4.3085 \times 10^{-5} T \ln \left(\frac{P_{H_2} \sqrt{P_{O_2}}}{P_{H_2O}} \right), \quad (5)$$

where P_{H_2} and P_{O_2} are the partial pressures of hydrogen and oxygen, respectively.

For a practical PEM electrolyzer, the cell voltage required in the electrolytic hydrogen process is always bigger than the reversible voltage owing to the existence of irreversibilities resulting mainly from the following three overpotential losses.

(1) The activation overpotential losses [19, 24-28]

$$V_{act} = \left(\frac{\alpha_A + \alpha_C}{\alpha_A \alpha_C} \right) \frac{RT}{2F} \ln\left(\frac{j}{j_0}\right), \tag{6}$$

where $j_0 = 1.08 \times 10^{-17} \exp(0.086T)$ is the exchange current density [27], j is the current density, R is the universal gas constant, F is Faraday's constant, and α_A and α_C are the charge transfer coefficients of the anode and cathode, respectively.

(2) The ohmic overpotential losses [19, 28-31]

$$V_{ohm} = j \frac{t_{mem}}{\sigma_{mem}}, \tag{7}$$

where t_{mem} is the membrane thickness, $\sigma_{mem} = (0.005139\lambda_{mem} - 0.003260) \exp[1268(\frac{1}{303} - \frac{1}{T})]$ is the conductivity of a Nafion membrane [31], $\lambda_{mem} = \begin{cases} 0.043 + 17.81a - 39.85a^2 + 36a^3, & 0 < a \leq 1, \\ 14 + 1.4(a - 1), & 1 < a \leq 3. \end{cases}$ is the membrane humidity [31, 32], $a = P_w / P_{sat}$ is the membrane water activity, P_w is the partial pressure of water vapor, and $P_{sat} = 1.01325 \times 10^{2.8206 + 0.02953(T - 273) - 9.1837 \times 10^{-5}(T - 273)^2 + 1.4454 \times 10^{-7}(T - 273)^3}$ is the water saturation pressure [26, 31, 33]. In a PEM electrolyzer, the membrane always operates under almost full humidification, i.e. $a = 1$ [33].

(3) The concentration overpotential losses [34]

$$V_{con} = j \left(\beta_1 \frac{j}{j_L} \right)^{\beta_2}, \tag{8}$$

where β_2 is a constant, j_L is the limiting current density, $\beta_1 = \begin{cases} (8.66 \times 10^{-5} T - 0.068) P_x - 1.6 \times 10^{-4} T + 0.54, & (P_x > 2) \\ (7.16 \times 10^{-4} T - 0.622) P_x - 1.45 \times 10^{-3} T + 1.68, & (P_x < 2) \end{cases}$, and $P_x = \frac{P_{O_2}}{0.1173 \times 101325} + \frac{P_{sat}}{101325}$.

García-Valverde et al. [24] used the above model to simulate the electrochemical, thermal, and H₂ output flow behaviours of the PEM electrolyzer. It was found that the simulation values are in good agreement with the experiment data [24]. It shows that the electrolyzer model adopted here is of practical significance.

Using the above equations, one can calculate the voltage and electric energy required by the PEM electrolyzer and the Joule heat produced in the PEM electrolyzer, which are, respectively, determined by

$$V = V_0 + V_{act} + V_{ohm} + V_{con} , \tag{9}$$

$$E = IV , \tag{10}$$

and

$$Q_J = I(V_{act} + V_{ohm} + V_{con}) , \tag{11}$$

where $I = jA_p$ is the electric current through the PEM electrolyzer and A_p is the effective surface area of the polar plate.

It is significant to note that the Joule heat produced in the PEM electrolyzer may be directly used to supply to the water splitting reactions and hence the heat input of the external heat source can be decreased. Thus, the thermal energy transferred from the external heat source to the electrolyzer may be reduced from Q to

$$Q_{PEM} = (Q - Q_J) . \tag{12}$$

According to Faraday’s law, the rate of electrochemical reaction ν depends on the operating electric current [35, 36], i.e.,

$$\nu = \pm \frac{dn}{dt} = \frac{I}{2F} , \tag{13}$$

where n is the number of moles and dn/dt is the molar consumption rate of H_2O . Based on Eq. (13), the outlet flow rates of H_2 , O_2 and H_2O are, respectively, given by

$$N_{H_2,out} = 2N_{O_2,out} = N_{H_2O,reacted} = \frac{I}{2F} \tag{14}$$

and

$$N_{H_2O,out} = N_{H_2O,in} - N_{H_2O,reacted} = N_{H_2O,in} - \frac{I}{2F} . \tag{15}$$

According to Fig. 1, the heat supplied by the external heat source to heat the compensatory water is given by:

$$\begin{aligned} Q_{H_2O} &= \frac{N_{H_2O,in}}{\varepsilon} \int_{T_0}^T C_{p,H_2O} dT - \left[N_{H_2,out} \int_{T_0}^T C_{p,H_2} dT + N_{O_2,out} \int_{T_0}^T C_{p,O_2} dT + N_{H_2O,out} \int_{T_0}^T C_{p,H_2O} dT \right] \\ &= \left[N_{H_2O,in} (1/\varepsilon - 1) + \frac{I}{2F} \right] \int_{T_0}^T C_{p,H_2O} dT - \frac{I}{2F} \int_{T_0}^T (C_{p,H_2} + \frac{C_{p,O_2}}{2}) dT , \end{aligned} \tag{16}$$

where ε is the effectiveness of the heat exchangers and $C_{p,i}$ ($i= \text{H}_2, \text{O}_2$ or H_2O) are the molar heat capacities of species i . It may be easily proved from Eq. (16) and the data in Table 1 [37-39] that $Q_{\text{H}_2\text{O}} > 0$.

Table 1. Thermodynamic parameters for the reactants/products at 101,325 Pa, where (g) and (l) refer to gas and liquid phases, respectively.

Compound	S(T0) (J mol ⁻¹ K ⁻¹)	Heat Capacity(C _{p,i}) (J mol ⁻¹ K ⁻¹)
H2 (g)	131	27.28+0.00326T+50000/T2
O2 (g)	205	29.96+0.00418T-167000/T2
H2O (l)	70	75.44

Table 2. Parameters used in the present modeling.

Parameter	Value
Faraday constant, F (C mol ⁻¹)	96,485
Universal gas constant, R (J mol ⁻¹ K ⁻¹)	8.314
Low heating value of H2, LHV (J mol ⁻¹)	241,830
Membrane thickness t_{mem} (m)	50×10 ⁻⁶
Transfer coefficient of the anode, α_A	0.5 [15]
Transfer coefficient of the cathode, α_C	1 [15]
Limiting current density, j_L (A m ⁻²)	20,000 [15]
Concentration overvoltage constant, β_2	2 [15]
Temperature of the electrolyzer, T (K)	363
Membrane water activity, a	1
Temperature of ambience, T_0 (K)	298.15
Temperature of heat source, T_s (K)	400
Partial pressure of hydrogen, P_{O_2} (Pa)	101,325
Partial pressure of oxygen, P_{H_2} (Pa)	101,325
Partial pressure of water, $P_{\text{H}_2\text{O}}$ (Pa)	101,325
Area of single-cell polar plate, A_p (m ²)	0.01
Flow rate of H2O at PEM inlet, $N_{\text{H}_2\text{O},in}$ (mol s ⁻¹)	0.001
Effectiveness of the heat exchangers, ε	0.7

Using the above equations and the data in Tables 1 and 2 [10, 26, 31, 40-43], we can obtain the curves of Q_k ($k=PEM$ and TE) varying with j , as shown in Fig. 2, where

$Q_{TE} = Q_{PEM}(1 - T_0/T) + Q_{H_2O}(1 - T_0/T_s)$ and j_Q is the current density when $Q_{TE} = 0$. It is clearly seen from Fig. 2 that when the PEM electrolyzer works at the temperatures between 353 K and 373 K, $Q_{PEM} < 0$, $Q_{TE} > 0$ in the region of $j < j_Q$ and $Q_{TE} < 0$ in the region of $j > j_Q$. When the operating temperature is increased, $|Q_{PEM}|$ decreases.

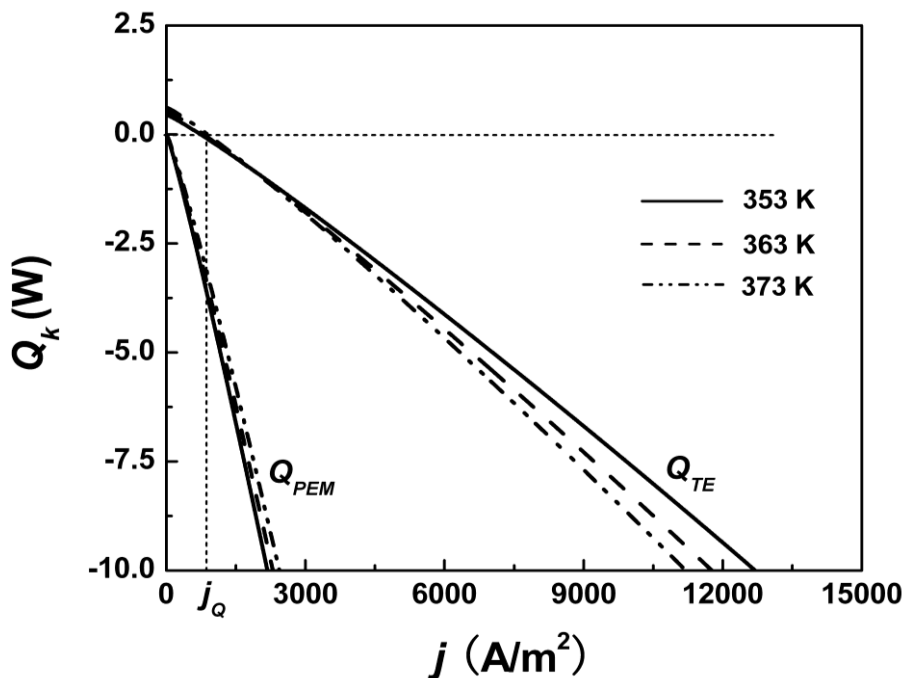
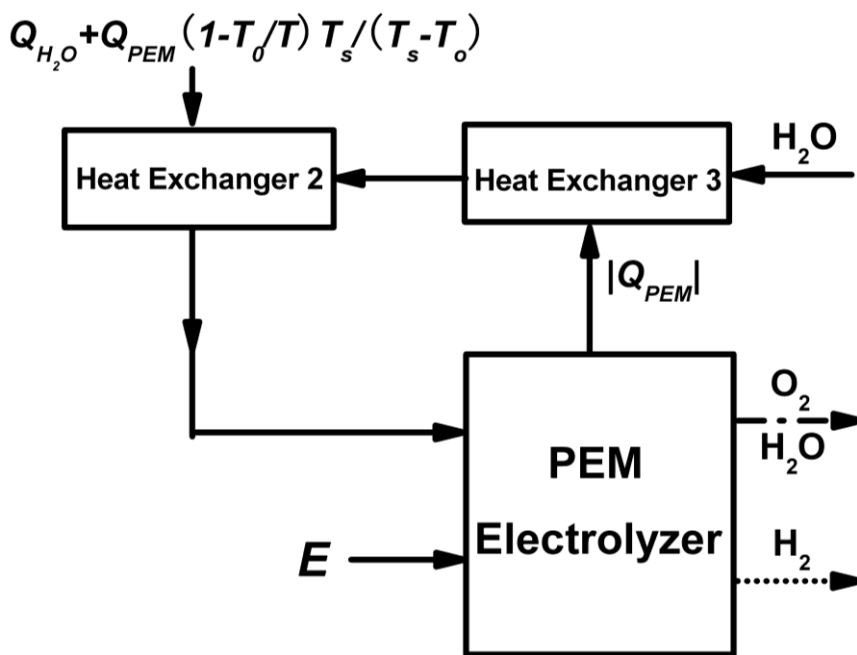


Figure 2. The curves of Q_{PEM} and Q_{TE} varying with the current density for different temperatures.



A

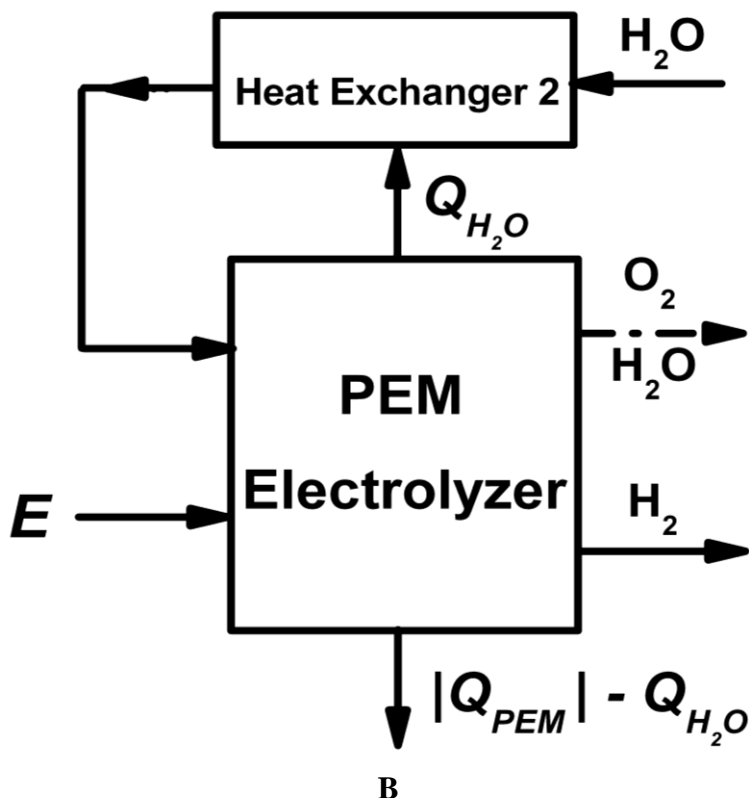


Figure 3. The part schematic diagrams of a PEM electrolyzer system for hydrogen production with (A) $Q_{TE} \geq 0$ and (B) $Q_{TE} < 0$. The other parts of the system are the same as those in Fig. 1

It is interesting to note that when $Q_{PEM} < 0$, besides Fig. 1, one can design some alternative configurations for a PEM electrolyzer system, as shown in Fig. 3. It is seen from Fig. 3(A) that when $Q_{PEM} < 0$ and $Q_{TE} \geq 0$, the redundant heat $|Q_{PEM}|$ generated in the PEM electrolyzer may be transferred to heat the water through an additional heat exchanger, i.e., heat exchanger 3. In such a case, $T_x = T$ and Eq. (1b) can be directly expressed as

$$\eta = \frac{N_{H_2,out} LHV}{E + Q_{PEM} (1 - \frac{T_0}{T}) + Q_{H_2O} (1 - \frac{T_0}{T_s})} \tag{17}$$

In Fig.3 (A), the heat $|Q_{PEM}|(1 - T_0/T)T_s / (T_s - T_0)$, which has the same temperature level as the external heat source connected to heat exchanger 2, is transferred to the water, so that the heat supplied by the external heat source can be reduced from Q_{H_2O} to $Q_{H_2O} - |Q_{PEM}|(1 - T_0/T)T_s / (T_s - T_0)$. It is seen from Fig. 3(B) that when $Q_{PEM} < 0$ and $Q_{TE} < 0$, one part of the redundant heat $|Q_{PEM}|$ may be used to replace the heat Q_{H_2O} supplied by the external heat source and to heat the water so that the temperature of the water attains that of the PEM electrolyzer, and the other part of the redundant heat $|Q_{PEM}|$ is

released to the environment. In such a case, neither Eq. (1b) nor Eq. (17) may be directly used to calculate the efficiency of the system, while the efficiency of the system should be expressed as

$$\eta = \frac{N_{H_2,out} LHV}{E} \tag{18}$$

In Fig. 3(B), the quantity of the heat transferred from the PEM electrolyzer to heat exchanger 2 is equal to $Q_{H_2O} = |Q_{PEM}|(1 - T_0/T)T_s / (T_s - T_0)$ and the quantity of the heat released to the environment is $|Q_{PEM}| - Q_{H_2O} = |Q_{PEM}|[1 - (1 - T_0/T)T_s / (T_s - T_0)]$.

4. EFFECTS OF SOME PARAMETERS ON THE EFFICIENCY

Unless otherwise described specifically, the following numerical calculations are performed based on the data in Tables 1 and 2 and Eqs. (3), (17) and (18). According to Figs. 1 and 3, one can generate some characteristic curves of the efficiency of the system varying with the current density under differently given parameters, as shown in Figs. 4 and 5.

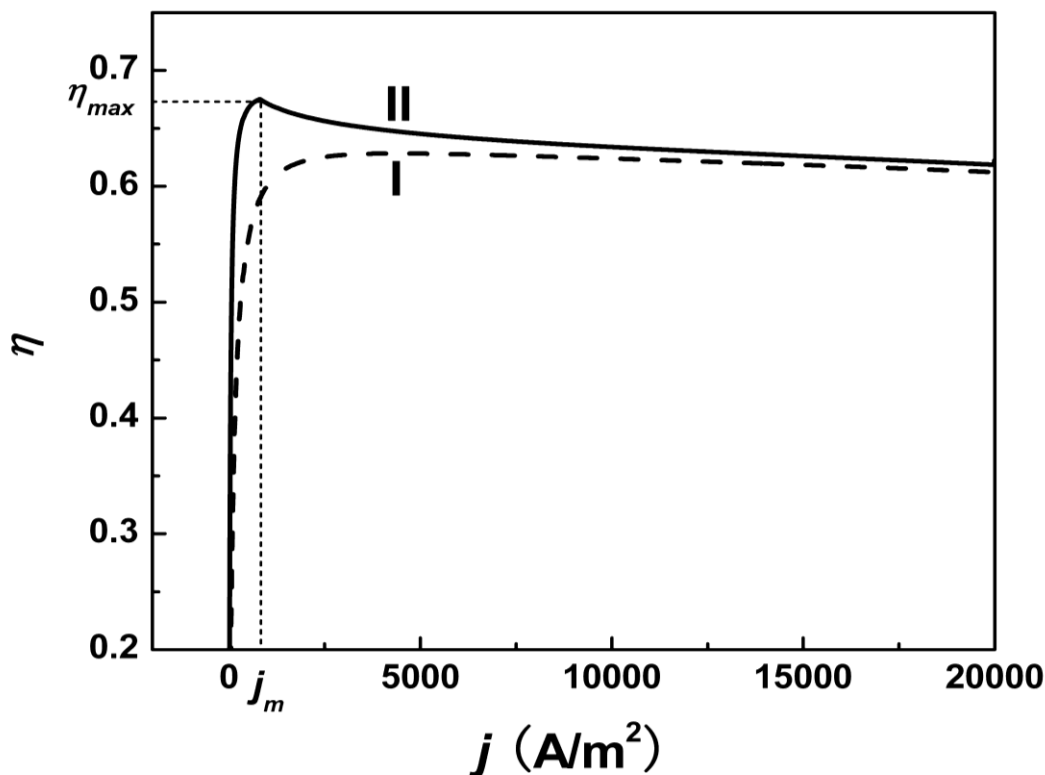
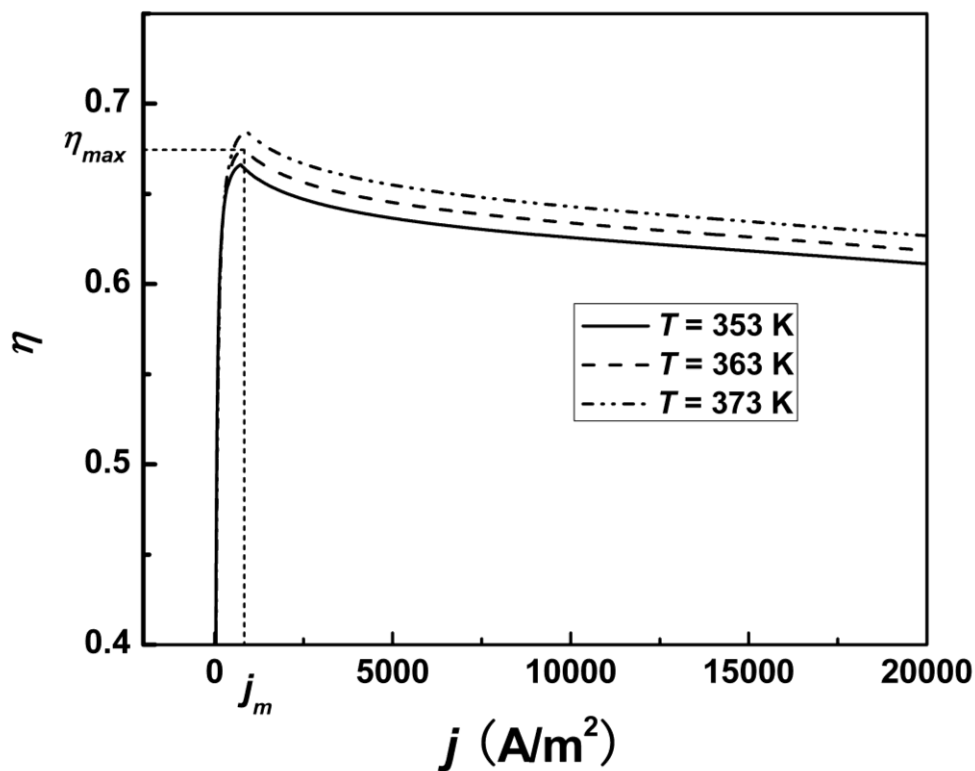
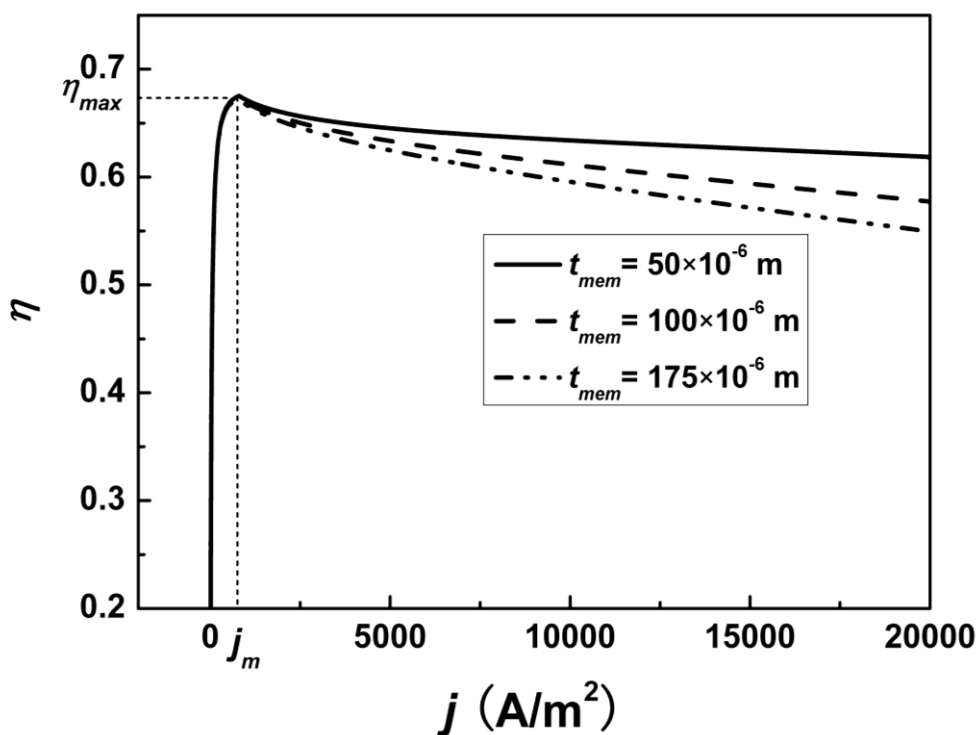


Figure 4. The curves of the efficiency of the system varying with the current density for different configurations. Curves I and II correspond to the configurations of Fig. 1 and Fig.3(A) and (B), respectively.

It is seen from Fig. 4 that when $Q_{PEM} < 0$, the efficiency of the system (Curve II) shown in Fig. 3 is higher than that (Curve I) shown in Fig. 1. It is taken for granted because the redundant heat $|Q_{PEM}|$ generated in the PEM electrolyzer is utilized in Fig. 3. Thus, in Fig. 5, we only discuss the performance of the system configurations shown in Fig. 3.



A



B

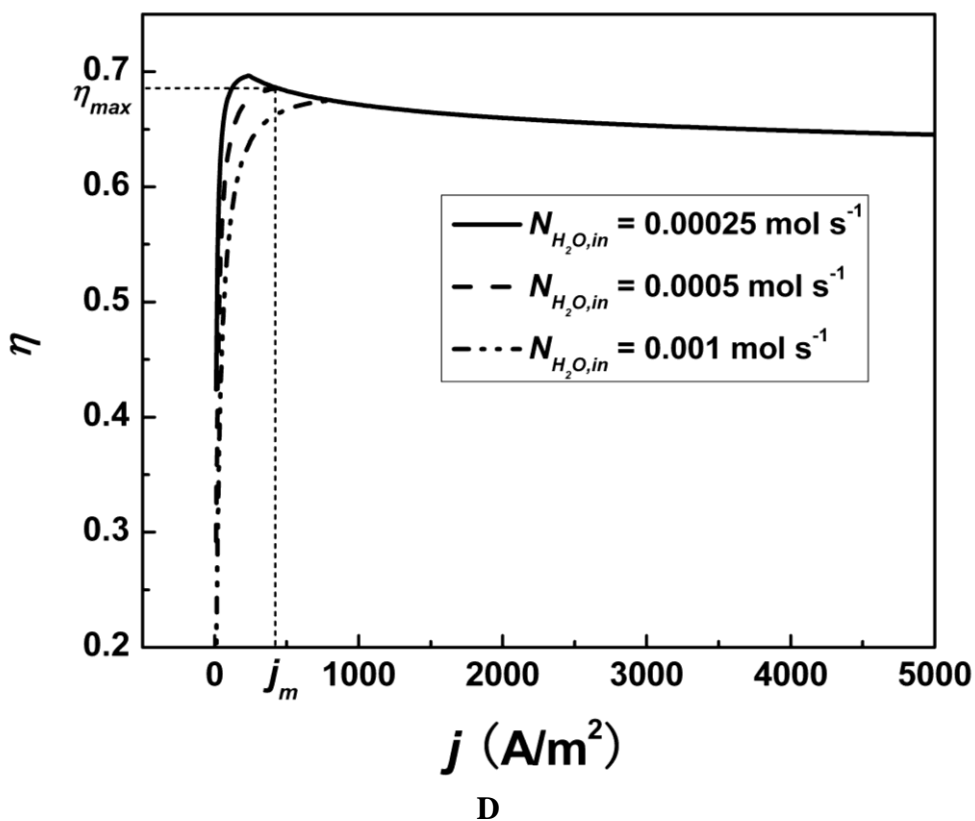
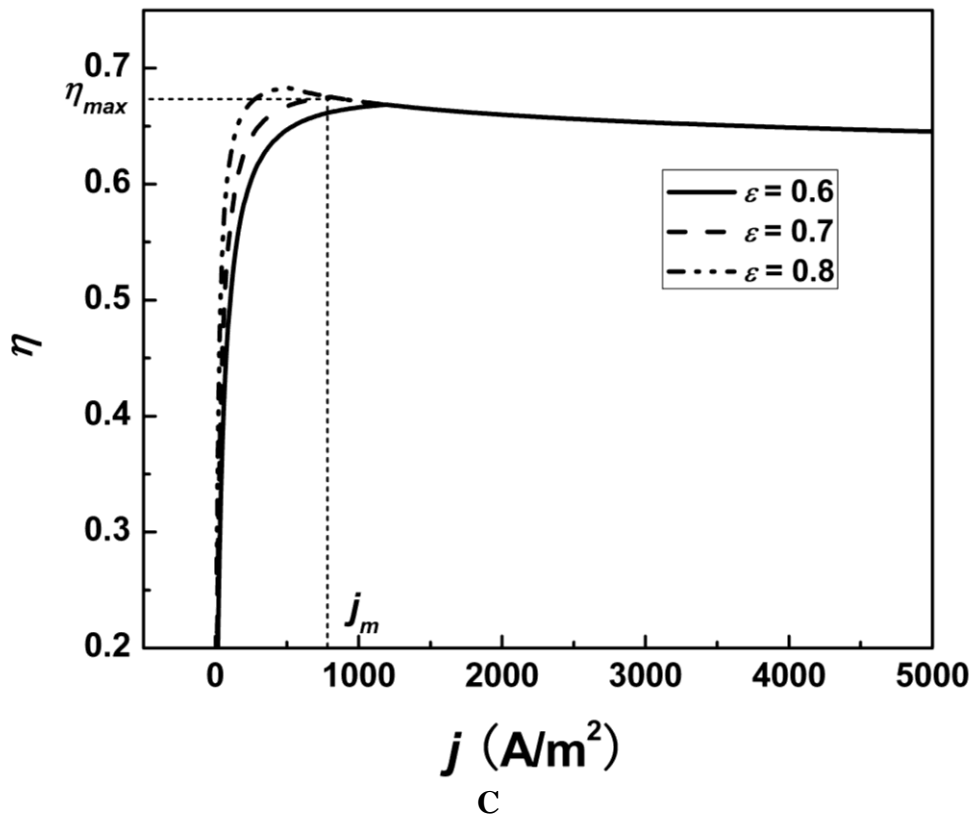


Figure 5. The efficiency versus current density curves for different (A) operating temperatures, (B) membrane thickness, (C) effectiveness of the heat exchangers, and (D) inlet flow rates of H₂O.

It is also seen from Fig. 4 that for a PEM electrolyzer system, there is a maximum efficiency η_{\max} and a corresponding current density j_m . The curves in Fig. 4 show clearly that in the region of $j < j_m$, the efficiency of the system decreases rapidly as the current density is decreased, as shown by the left side of curve II which is generated by Eq. (17) corresponding to Fig. 3(A); while in the region of $j > j_m$, the efficiency of the system increases as the current density is decreased, as shown by the right side of curve II which is generated by Eq. (18) corresponding to Fig. 3(B). When $j = j_m$, Eq. (17) is equal to Eq. (18) and j_m is equal to j_Q in Fig. 2. It means the fact that one should choose the configuration shown in Fig. 3(B) so that the PEM electrolyzer system is operated in the region of $j \geq j_m$. For the parameters given in Table 2, the value of j_m is equal to 806 A/m^2 . It should be pointed out that j_m is the lowest bound of the optimized current density. In order to obtain a larger hydrogen production rate, the current densities in the practical PEM electrolyzer systems [16, 44, 45] are usually chosen to be much larger than j_m , which is in agreement with the optimal condition of the current density.

The influence of the operating temperature on the performance of the system is shown in Fig. 5(A). When $j \geq j_m$, the efficiency of the electrolysis system increases as the operating temperature is increased. Moreover, the maximum efficiency and the current density corresponding to the maximum efficiency increase monotonically with the increasing of the operating temperature.

The influence of the electrolyte membrane thickness on the performance of the system in the optimal current density region is shown in Fig. 5(B). It shows that the efficiency of the electrolysis system decreases as the electrolyte membrane thickness is increased. Furthermore, the influence of the electrolyte membrane thickness on the efficiency of the system increases as the current density is increased.

The influence of the effectiveness of the heat exchangers on the performance of the system is shown in Fig. 5(C). The efficiency of the system increases as the effectiveness of the heat exchangers is increased. However, the influence mainly happens in the region of $j \leq j_m$. When $j > j_m$, the redundant heat generated in the electrolyzer $|Q_{PEM}|$ is larger than the thermal energy Q_{H_2O} needed from the external heat sources, so that the influence of the effectiveness of the heat exchangers can be neglected.

The influence of the inlet flow rate of water on the performance of the electrolysis system is shown in Fig. 5(D). It shows that the efficiency of the system decreases as the inlet flow rate of water is increased. Similarly, the influence mainly happens in the region of $j \leq j_m$, and this influence can be negligible in the other regions.

5. CONCLUSIONS

A PEM water electrolysis system for hydrogen production is established and the efficiencies of the system are given for the cases of $Q_{PEM} \geq 0$ and $Q_{PEM} < 0$. Based on semi-empirical equations, the irreversible losses in a PEM water electrolysis process are calculated. It shows that in the whole operating current density range, $Q_{PEM} < 0$. Some alternative configurations for utilizing the redundant heat resulting from the PEM electrolyzer are put forward to improve the performance of the system. It

is found that the efficiencies of the alternative configurations are higher than those that the redundant heat is directly released into the environment. It is expounded that the operating current density for the alternative configurations should be situated in the region $j > j_m$. Moreover, it is revealed that the efficiency of the system increases as the operating temperature and the effectiveness of the heat exchangers are increased and decreases as the electrolyte membrane thickness and the inlet flow rate of H₂O are increased. The optimum design strategies obtained here may enrich thermodynamic and electrochemical theories of a PEM electrolyzer and provide some guidance for the optimum design and operation of practical PEM electrolysis systems for hydrogen production.

ACKNOWLEDGMENTS

This work was supported by the Fujian Natural Science Foundation and the Fundamental Research Fund for the Central Universities (No. 201112G006), People's Republic of China.

References

1. Y. Kiros, *Int. J. Electrochem. Sci.*, 2(2007)285.
2. M. Perez-Page, V. Perenz-Herranz, *Int. J. Electrochem. Sci.*, 6(2011)492.
3. C. M. Bautista-Rodríguez, M. G. A. Rosas-Paletta, J. A. Rivera-Marquez, N. Tepale-Ochoa, *Int. J. Electrochem. Sci.*, 6(2011)256.
4. V. A Goltsov, T. N. Veziroglu, *Int. J. Hydrogen Energy*, 26 (2001) 909.
5. H. S. Roh, D. K. Lee, K. Y. Koo, U. H. Jung, W. L. Yoon, *Int. J. Hydrogen Energy*, 35 (2010) 1613.
6. M. Ni, M. K. H. Leung, D. Y. C. Leung, *J. Power Sources*, 163 (2006) 460.
7. C. Wu, Q. Huang, M. Sui, Y. Yan, F. Wang, *Fuel Process. Technol.*, 89 (2008) 1306.
8. M. A. Rosen, *Energy*, 35 (2010) 1068.
9. H. Zhang, S. Su, G. Lin, J. Chen. *Int. J. Electrochem. Sci.*, 6 (2011) 2566.
10. M. Ni, M. K. H. Leung, D. Y. C. Leung, *Energy Convers. Manage.*, 49 (2008) 2748.
11. O. F. Selamet, F. Becerikli, M. D. Mat, Y. Kaplan, *Int. J. Hydrogen Energy*, 36 (2011) 11480.
12. A. Marshall, B. Borresen, G. Hagen, M. Tsytkin, R. Tunold, *Energy*, 32 (2007) 431.
13. S. Siracusano, V. Baglio, A. D. Blasi, N. Briguglio, A. Stassi, R. Ornelas, et al., *Int. J. Hydrogen Energy*, 35 (2010) 5558.
14. K. Naga Mahesh, J. Sarada Prasad, M. Venkateswer Rao, V. Himabindu, A. Yerramilli, P. Raghunathan Rao, *Int. J. Hydrogen Energy*, 34 (2009) 6085.
15. A. T. Marshall, S. Sunde, M. Tyskin, R. Tunold, *Int. J. Hydrogen Energy*, 32 (2007) 2320.
16. S. P. S. Badwal, S. Giddey, F. T. Ciacchi, *Ionics*, 12 (2006) 7.
17. P. Millet, R. Ngameni, S. A. Grigoriev, N. Mbemba, F. Brisset, A. Ranjbari, C. Etiévant. *Int. J. Hydrogen Energy*, 34 (2009)1.
18. K. W. Harrison, E. H. Pacheco, M. Mann, H. Salefhar, *J. Fuel Cell Sci. Technol.*, 3 (2006) 220.
19. F. Marangio, M. Santarelli, M. Cali, *Int. J. Hydrogen Energy*, 34 (2009) 1143.
20. M. A. Rosen, *Int. J. Hydrogen Energy*, 20 (1995) 547.
21. R. L. LeRoy, C. T. Bowen, D. J. LeRoy, *J. Electrochem. Soc.*, 127 (1980) 1954.
22. R. Balaji, N. Senthil, S. Vasudevan, S. Ravichandran, S. Mohan, et al., *Int. J. Hydrogen Energy*, 36 (2011) 1399.
23. T. Oi, Y. Sakaki, *J. Power Sources*, 129 (2004) 229.
24. R. García-Valverde, N. Espinosa, A. Urbina, *Int. J. Hydrogen Energy*, 2012, 37: 1927.
25. A. Yilanci, I. Dincer, H. K. Ozturk, *Int. J. Hydrogen Energy*, 33 (2008) 7538.

26. M. Ay, A. Midilli, I. Dincer, *Int. J. Energy Research*, 30 (2006) 307.
27. S. O. Mert, I. Dincer, Z. Ozcelik, *J. Power Sources*, 165 (2007) 244.
28. T. A. Zawodzinski, C. Derouin, S. Radzinski, R. J. Sherman, V. T. Smith, T. A. Springer, et al., *J. Electrochem. Soc.*, 140 (1993) 1041.
29. H. Görgün, *Int. J. Hydrogen Energy*, 31 (2006) 29.
30. R. García-Valverde, N. Espinosa, A. Urbina, *Int. J. Hydrogen Energy*, 36 (2011) 10574.
31. T. E. Springer, T. A. Zawodzinski, S. Gottesfeld, *J. Electrochem. Soc.*, 138 (1991) 2334.
32. V. Gurau, F. Barbir, H. Liu, *J. Electrochem. Soc.*, 147 (2000) 2468.
33. R. O'Hayre, S. W. Cha, W. Colella, F. B. Prinz, *Fuel cell fundamentals*, John Wiley & Sons, Ltd., New York (2006).
34. J. Nieminen, I. Dincer, G. Naterer, *Int. J. Hydrogen Energy*, 35 (2010) 10842.
35. Y. Zhao, C. Ou, J. Chen, *Int. J. Hydrogen Energy*, 33 (2008) 4161.
36. S. J. Watowich, R. S. Berry, *J. Phys. Chem.*, 90 (1986) 4624.
37. Y. Shin, W. Park, J. Chang, J. Park, *Int. J. Hydrogen Energy*, 32 (2007) 1486.
38. H. Zhang, G. Lin, J. Chen, *Int. J. Hydrogen Energy*, 35 (2010) 10851.
39. H. Zhang, G. Lin, J. Chen, *Int. J. Hydrogen Energy*, 36 (2011) 4015.
40. A. Rowe, X. G. Li, *J. Power Sources*, 102 (2001) 82.
41. J. Hamelin, K. Agbossou, A. Laperrière, F. Laurencelle, T. K. Bose, *Int. J. Hydrogen Energy*, 26 (2001) 625.
42. M. Ni, M. K. H. Leung, D. Y. C. Leung, Electrochemistry modeling of proton exchange membrane (PEM) water electrolysis for hydrogen production. Lyon, France, WHEC 2006, 13-16 June, 2006.
43. T. Ioroi, K. Yasuda, Z. Siroma, N. Fujiwara, Y. Miyazaki, *J. Power Sources*, 112 (2002) 583.
44. F. Barbir, *Solar Energy*, 78 (2005) 661.
45. S. A. Grigoriev, V. I. Poremsky, V. N. Fateev, *Int. J. Hydrogen Energy*, 31 (2006) 171.